

PITHA 98/21  
July 02, 1998

# Measurement of $C$ -Parameter and Determination of $\alpha_s$ from $C$ -Parameter and Jet Broadening at PETRA Energies

P.A. Movilla Fernández<sup>(1)</sup>, O. Biebel<sup>(1)</sup>, S. Bethke<sup>(1)</sup>  
and the JADE Collaboration<sup>(2)</sup>

## Abstract

$e^+e^-$  annihilation data recorded by the JADE detector at PETRA were used to measure the  $C$ -parameter for the first time at  $\sqrt{s} = 35$  and 44 GeV. The distributions were compared to a resummed QCD calculation which recently became available for this observable. In addition, we applied extended resummed calculations to the heavy and wide jet broadening variables,  $B_T$  and  $B_W$ , which now include a proper treatment of the quark recoil against multi-gluon emission with single-logarithmic accuracy. We further investigated power corrections to the mean values of the observables mentioned above. In this study, we considered all available  $e^+e^-$  data between  $\sqrt{s} = 35$  and 172 GeV.

<sup>(1)</sup> III. Physikalisches Institut der RWTH Aachen, D-52056 Aachen, Germany  
contact e-mail: Otmar.Biebel@Physik.RWTH-Aachen.DE

<sup>(2)</sup> for a full list of members of the JADE Collaboration see Reference [1]

# 1 Introduction

In a recent publication [2] we have presented a study of event shapes observables and determinations of  $\alpha_s$  using data of  $e^+e^-$  annihilations at  $\sqrt{s} = 22$  to  $44$  GeV recorded with the former JADE detector [3] at the PETRA collider. This study provided valuable information which was not available before from  $e^+e^-$ -annihilations in the PETRA energy range. The results on  $\alpha_s$ , obtained in a similar manner as those from the experiments at LEP, demonstrated that the energy dependence of  $\alpha_s(Q)$  is in good agreement with the prediction of Quantum Chromodynamics (QCD). Evolved to the  $Z^0$  mass scale, the results are in good agreement with those obtained at LEP, and are of similar precision. In addition, power corrections, applied to analytic QCD calculations of the mean values of event shape distributions, were found to qualitatively and quantitatively match the effects of hadronisation. Thus QCD could be tested without the need of phenomenological hadronisation models.

Meanwhile the perturbative calculations for the jet broadening variables were improved by including a proper treatment of quark recoil [4]. Furthermore for the  $C$ -parameter a resummation of leading and next-to-leading logarithm terms to all orders of  $\alpha_s$  (NLLA) became available [5]. Beside these advances in the perturbative description of event shape observables progress was made in the understanding of non-perturbative power corrections to the event shape observables and their mean values. In particular two-loop calculations of such corrections were performed [6] which modify the one-loop result of the power correction to the event shapes by a factor (Milan factor).

In this paper we complement our previous publication by a new  $\mathcal{O}(\alpha_s^2)$ +NLLA determination of  $\alpha_s$  from  $C$ -parameter and update the determination from jet broadening at  $\sqrt{s} = 35$  and  $44$  GeV in the Sections 3 and 4. We also applied power corrections to the  $C$ -parameter distributions and re-investigated those for the mean values of the thrust, heavy jet mass and both jet broadening observables in Section 5. We start in Section 2 with a brief summary of the data samples used and draw conclusions from our results in Section 6.

## 2 Data samples and Monte Carlo simulation

We analysed data recorded with the JADE detector in 1984 to 1986 at centre-of-mass energies of  $39.5$ - $46.7$  GeV and around  $35$  GeV. The JADE detector was operated from 1979 until 1986 at the PETRA electron-positron collider at centre-of-mass energies of  $\sqrt{s} = 12$  to  $46.7$  GeV.

A detailed description of the JADE detector can be found in [1, 3]. The main components of the detector were the central jet chamber to measure charged particle tracks and the lead glass calorimeter to measure energy depositions of electromagnetic showers, which both covered almost the whole solid angle of  $4\pi$ .

Multihadronic events were selected by the standard JADE selection cuts [7]. All charged particle tracks, assumed to be pions, with a total momentum of  $|\vec{p}| > 100$  MeV/ $c$  were considered in the analysis. Energy clusters in the electromagnetic calorimeter, assumed to be photons, were considered if their energies exceeded 150 MeV after correction

year	$\sqrt{s}$ [GeV]	data	MC
1984/85	40-48	6158	14 497
1986	35	20 926	25 123

Table 1: Number of events in data and in Monte Carlo detector simulation retained after application of the multihadron selection cuts described in the text.

for energy deposited by associated tracks.

Background from two-photon processes and  $\tau$ -pair events and from events with hard initial state photon radiation were removed by cuts on the visible energy  $E_{\text{vis}} = \sum E_i$ , the total missing momentum  $p_{\text{miss}} = |\sum \vec{p}_i|$  ( $\vec{p}_i$  and  $E_i$  are the 3-momentum and the energy of the tracks and clusters), the longitudinal balance relative to the  $e^+e^-$  beam axis of momenta  $p_{\text{bal}} = |\sum p_i^z/E_{\text{vis}}|$  and the polar angle of the thrust axis,  $\theta_T$ :

- $E_{\text{vis}} > \sqrt{s}/2$  ;
- $p_{\text{miss}} < 0.3 \cdot \sqrt{s}$  ;
- $p_{\text{bal}} < 0.4$  ;
- $|\cos \theta_T| < 0.8$  .

Thus the backgrounds from  $\gamma\gamma$  and  $\tau$ -pair events were reduced to less than 0.1% and 1%, respectively [8]. The numbers of events which were retained after these cuts for this analysis are listed in Table 1.

Corresponding original Monte Carlo detector simulation data for 35 and 44 GeV were based on the QCD parton shower event generator JETSET 6.3 [10]. These original Monte Carlo events at 35 GeV had the coherent branching for the parton shower while the 44 GeV events had non-coherent branching<sup>1</sup>. The main parameters used for event generation are given in Section 3.2. Both samples included a simulation of the acceptance and resolution of the JADE detector.

### 3 Experimental procedure

From the data samples described in the previous section, the event shape distribution of the  $C$ -parameter was determined. The  $C$ -parameter is defined as [11]

$$C = 3(\lambda_1\lambda_2 + \lambda_2\lambda_3 + \lambda_3\lambda_1)$$

where  $\lambda_\gamma$ ,  $\gamma = 1, 2, 3$ , are the eigenvalues of the momentum tensor

$$\Theta^{\alpha\beta} = \frac{\sum_i \vec{p}_i^\alpha \vec{p}_i^\beta / |\vec{p}_i|}{\sum_j |\vec{p}_j|} .$$

---

<sup>1</sup>The different treatment of coherence in these samples of simulated data has no visible influence on the results of this study.

### 3.1 Correction procedure

Limits of the detector's acceptance and resolution and effects due to initial state photon radiation were corrected by applying a bin-by-bin correction procedure to the event shape distributions. The correction factors were defined by the ratio of the distribution calculated from events generated by JETSET 6.3 at *hadron level* over the same distribution at *detector level*. The *hadron level* distributions were obtained from JETSET 6.3 generator runs without detector simulation and without initial state radiation, using all particles with lifetimes  $\tau > 3 \cdot 10^{-10}$  s. Events at *detector level* contained initial state photon radiation and a detailed simulation of the detector response, and were processed in the same way as the data.

Next, the data distributions were further corrected for hadronisation effects. This was done by applying bin-by-bin correction factors derived from the ratio of the distribution at *parton level* over the same distribution at *hadron level*, which were calculated from JETSET generated events before and after hadronisation, respectively. The correction factors are typically of the order 10 to 20% growing large towards the 2-jet region. In the case of the  $C$ -parameter the correction factors are also large next to the 3-jet boundary which is at  $C = 0.75$ . The data distributions, thus corrected to the *parton level*, can be compared to analytic QCD calculations.

### 3.2 Systematic uncertainties

Systematic uncertainties of the corrected data distributions were investigated by modifying details of the event selection and of the correction procedure. For each variation the whole analysis was repeated and any deviation from the main result was considered a systematic error. In general, the maximum deviation from the main result for each kind of variation was regarded as symmetric systematic uncertainty. The main result was obtained using the default selection and correction procedure as described above.

In detail, we considered either tracks or clusters only for the measurement of the event shape distributions. We varied the cut on  $\cos \theta_T$  by  $\pm 0.1$ . The cut on  $p_{\text{miss}}$  was either removed or tightened to  $p_{\text{miss}} < 0.25 \cdot \sqrt{s}$ . Similarly, the momentum balance requirement was either restricted to  $p_{\text{bal}} < 0.3$  or dropped. We also varied the cut for the visible energy  $E_{\text{vis}}$  by  $\pm 0.05 \cdot \sqrt{s}$ . In order to check the residual contributions from  $\tau$ -pair events we also required at least seven well-measured charged tracks.

To study the impact of the hadronisation model of the JETSET 6.3 generator, the values of several significant model parameters were varied around their tuned values from Reference [12] used for our main result. Different sets of correction factors to correct the data from *hadron level* to *parton level* were generated by varying single parameters of the JETSET generator. The variations were chosen to be similar to the one standard deviation percentage limits obtained by the OPAL Collaboration from a parameter tuning of JETSET at  $\sqrt{s} = M_{Z^0}$  [13]. In detail, we investigated the effects due to parton shower, hadronisation parameters, and quark masses. The amount of gluon radiation during the parton shower development was modified by varying  $\Lambda_{\text{LLA}}$  by  $\pm 50$  MeV around the tuned value 400 MeV. To vary the onset of hadronisation, we altered the parton shower cut-off parameter  $Q_0$  by  $\pm 0.5$  GeV around the tuned value of 1 GeV. We used the full

observed variation of  $\alpha_s$  to reflect a variation of  $Q_0$  between 0 and 2 GeV. The width  $\sigma_0 = 300$  MeV of the transverse momentum distribution in the hadronisation process was varied by  $\pm 30$  MeV. The LUND symmetric fragmentation function, applied to hadronise events of up, down and strange quarks, was varied by changing the  $a$  parameter from 0.5 by  $\pm 0.225$  whereas the  $b$  parameter was kept fixed at 0.9. As a systematic variation we used the LUND [10] instead of the Peterson et al. [14] fragmentation function for charm and bottom quarks. The effects due to the bottom quark mass were studied by restricting the model calculations which were used to determine the correction factors to up, down, strange, and charm quarks (udsc) only. Any deviation from our main result due to mass effects was treated as asymmetric error.

## 4 Determination of $\alpha_s$

### 4.1 Corrected event shape distributions

After applying the corrections for detector and for initial state radiation effects we obtained the  $C$ -parameter event shape distributions at *hadron level*. In Tables 3 the corrected data values are listed with statistical errors and experimental systematic uncertainties. The mean values of the distributions are also given. Our measured results for the jet broadening event shape distributions can be found in Ref. [2].

### 4.2 Determination of $\alpha_s$ using $\mathcal{O}(\alpha_s^2)$ +NLLA calculations

We determined  $\alpha_s$  by  $\chi^2$  fits to event shape distributions of  $C$  and also  $B_T$  and  $B_W$  corrected to the *parton level*. For the sake of direct comparison to other published results we chose the so-called  $\ln(R)$ -matching scheme to merge the  $\mathcal{O}(\alpha_s^2)$  with the NLLA calculations. The fits to the  $C$ -parameter distributions applied the resummation results obtained in [5]. For the fits to the jet broadening measures we used the improved calculation of Ref. [4] which includes a proper treatment of the quark recoil against an ensemble of soft gluons that is essential in the calculation of the jet broadening distributions. The renormalisation scale factor,  $x_\mu \equiv \mu/\sqrt{s}$ , was set to  $x_\mu = 1$  for the main result. Here, the value of  $\mu$  defines the energy scale at which the theory is renormalised.

The fit ranges for each observable were determined by choosing the largest range for which the hadronisation uncertainties remained below about 10 %, for which the  $\chi^2/\text{d.o.f.}$  of the fits did not exceed the minimum by more than a factor of two, and by aiming at results for  $\alpha_s$  that are independent from changes of the fit range. The remaining changes when enlarging or reducing the fit range by one bin on either side were taken as systematic uncertainties. Only statistical errors were considered in the fit thus resulting in  $\chi^2/\text{d.o.f.}$  larger than unity. The finally selected fit ranges, the  $\alpha_s$  results of the  $\chi^2$  fits and of the study of systematic uncertainties are tabulated in Tables 4 and 5, and are shown in Figures 1 and 2.

We also changed the renormalisation scale factor in the range of  $x_\mu = 0.5$  to 2.0. We found variations larger than the uncertainties from the detector correction and the hadronisation model dependence. The dependence of the fit result for  $\alpha_s$  on  $x_\mu$  indicates the importance of higher order terms in the theory.

It should be pointed out that the improved perturbative calculation for the jet broadening resulted in a larger  $\alpha_s$  value from the fit to the data. The systematic uncertainties are not affected by the new calculation but the  $\chi^2$  improved slightly.

We combined these new results with the  $\alpha_s$  results of our previous publication [2] replacing the results obtained from the jet broadening observables. A single  $\alpha_s$  value was obtained from the individual determinations from thrust, heavy jet mass, total and wide jet broadening,  $C$ -parameter and differential 2-jet rate following the procedure described in References [9, 15, 16]. This procedure accounts for correlations of the systematic uncertainties. At each energy, a weighted average of the six  $\alpha_s$  values was calculated with the reciprocal of the square of the respective total error used as a weight. In the case of asymmetric errors we took the average of the positive and negative error to determine the weight. For each of the systematic checks, the mean of the  $\alpha_s$  values from all considered observables was determined. Any deviation of this mean from the weighted average of the main result was taken as a systematic uncertainty.

With this procedure we obtained as final results for  $\alpha_s$

$$\begin{aligned}\alpha_s(35 \text{ GeV}) &= 0.1448 \pm 0.0017(\text{stat.}) {}^{+0.0117}_{-0.0069}(\text{syst.}) \\ \alpha_s(44 \text{ GeV}) &= 0.1392 \pm 0.0017(\text{stat.}) {}^{+0.0104}_{-0.0072}(\text{syst.}) .\end{aligned}$$

The systematic errors at 35 and 44 GeV are the quadratic sums of the experimental uncertainties ( $\pm 0.0017$ ,  $\pm 0.0032$ ), the effects due to the Monte Carlo modelling ( ${}^{+0.0070}_{-0.0035}$ ,  ${}^{+0.0050}_{-0.0027}$ ) and the contributions due to the variation of the renormalisation scale ( ${}^{+0.0092}_{-0.0057}$ ,  ${}^{+0.0086}_{-0.0058}$ ). It should be noted that the modelling uncertainties due to quark mass effects contribute significantly to the total error.

## 5 Mean Values of Distributions and QCD Power Corrections

### 5.1 Power corrections

The value of  $\alpha_s$  can also be assessed by the energy dependence of mean values of event shape distributions. Perturbative calculations exist for the mean values of thrust, heavy jet mass, total and wide jet broadening and  $C$ -parameter up to  $\mathcal{O}(\alpha_s^2)$ . An observable  $\mathcal{F}$  is given by the expression

$$\langle \mathcal{F}^{\text{pert.}} \rangle = A_{\mathcal{F}} \left( \frac{\alpha_s}{2\pi} \right) + (B_{\mathcal{F}} - 2A_{\mathcal{F}}) \left( \frac{\alpha_s}{2\pi} \right)^2$$

where the coefficients  $A_{\mathcal{F}}$  and  $B_{\mathcal{F}}$  were determined from the  $\mathcal{O}(\alpha_s^2)$  perturbative calculations [17–20]. The term  $-2A_{\mathcal{F}}$  accounts for the difference between the total cross-section used in the measurement and the Born level cross-section used in the perturbative calculation. The numerical values of these coefficients are summarised in Table 2.

In this study we corrected for hadronisation effects by additive power-suppressed corrections ( $1/\sqrt{s}$ ) to the perturbative predictions of the mean values of the event shape observables. The non-perturbative effects are due to the emission of very low energetic

Observable $\mathcal{F}$	$A_{\mathcal{F}}$	$B_{\mathcal{F}}$	$a_{\mathcal{F}}$
$\langle T \rangle$	2.103	44.99	-1
$\langle M_H^2/s \rangle$	2.103	23.24	0.5
$\langle B_T \rangle$	4.066	64.24	0.5
$\langle B_W \rangle$	4.066	-9.53	0.25
$\langle C \rangle$	8.638	146.8	$3\pi/2$

Table 2: Coefficients of the perturbative prediction [17–20] and coefficients and parameters of the power corrections [6] to the mean values of the event shape observables. Note that the definition of  $a_{\mathcal{F}}$  does not include the  $2\mathcal{M}/\pi$  factor introduced in [6].

gluons which can not be treated perturbatively due to the divergence of the perturbative expressions for  $\alpha_s$  at low scales. In the calculations of Reference [21] and also [6] which we used in this analysis a non-perturbative parameter

$$\bar{\alpha}_0(\mu_I) = \frac{1}{\mu_I} \int_0^{\mu_I} dk \alpha_s(k)$$

was introduced to replace the divergent portion of the perturbative expression for  $\alpha_s(\sqrt{s})$  below an infrared matching scale  $\mu_I$ . The general form of the power correction to the mean value of an observable  $\mathcal{F}$  was first given in Reference [21]. It was the result of a one-loop calculation. In References [6] similar calculations have been performed at two-loops. It could be shown that the two-loop result modifies the one-loop result only by a factor  $\mathcal{M} \approx 1.8$  which is known at the Milan factor. An additional factor  $2/\pi$  is due to the different definitions of the non-perturbative parameters  $\alpha_{\text{eff}}$ , being the so-called “effective coupling” [22], and  $\bar{\alpha}_0$  as defined above.

The two-loop result for the power correction assumes for thrust, heavy jet mass and  $C$ -parameter the form [6]

$$\begin{aligned} \langle \mathcal{F}^{\text{pow.}} \rangle = & a_{\mathcal{F}} \frac{4C_F}{\pi} \cdot \frac{2\mathcal{M}}{\pi} \cdot \left( \frac{\mu_I}{\sqrt{s}} \right) \cdot \\ & \cdot \left[ \bar{\alpha}_0(\mu_I) - \alpha_s(\sqrt{s}) - \frac{\beta_0}{2\pi} \left( \ln \frac{\sqrt{s}}{\mu_I} + \frac{K}{\beta_0} + 1 \right) \alpha_s^2(\sqrt{s}) \right], \end{aligned}$$

where  $C_F = 4/3$ , while for the two jet broadening measures the correction is logarithmically enhanced by a factor  $\ln(\sqrt{s}/Q_B)$ . We approximated  $Q_B$  by  $\mu_I$  such that

$$\begin{aligned} \langle \mathcal{F}^{\text{pow.}} \rangle = & a_{\mathcal{F}} \frac{4C_F}{\pi} \cdot \frac{2\mathcal{M}}{\pi} \cdot \left( \frac{\mu_I}{\sqrt{s}} \right) \cdot \ln \left( \frac{\sqrt{s}}{\mu_I} \right) \cdot \\ & \cdot \left[ \bar{\alpha}_0(\mu_I) - \alpha_s(\sqrt{s}) - \frac{\beta_0}{2\pi} \left( \ln \frac{\sqrt{s}}{\mu_I} + \frac{K}{\beta_0} + 1 \right) \alpha_s^2(\sqrt{s}) \right]. \end{aligned}$$

Using this approximation an extra correction without the logarithmic enhancement [6] was left out because it is small and strongly anti-correlated to the enhanced correction. Furthermore we found that the available data on the jet broadening are not yet sensitive to this extra correction.

The factor  $\beta_0 = (11C_A - 2N_f)/3$  in the two expressions stems from the QCD  $\beta$ -function of the renormalisation group equation. It depends on the number of colours,  $C_A = 3$ , and number of active quark flavours  $N_f$ , for which we used  $N_f = 5$  throughout the analysis. The term  $K = (67/18 - \pi^2/6)C_A - 5/9 \cdot N_f$  originates from the choice of the  $\overline{\text{MS}}$  renormalisation scheme. The remaining coefficient  $a_{\mathcal{F}}$  is listed in Table 2 for the event shapes considered.

## 5.2 Determination of $\alpha_s$ using power corrections

We determined  $\alpha_s(M_{Z^0})$  by  $\chi^2$  fits of the expression

$$\langle \mathcal{F} \rangle = \langle \mathcal{F}^{\text{pert.}} \rangle + \langle \mathcal{F}^{\text{pow.}} \rangle.$$

to the mean values of the five observables, thrust, heavy jet mass,  $C$ -parameter, and total and wide jet broadening, including the measured mean values obtained by other experiments at different centre-of-mass energies [23–26]. For the central values of  $\alpha_s$  from the fits we chose a renormalisation scale factor of  $x_\mu = 1$  and an infrared scale of  $\mu_I = 2$  GeV. The  $\chi^2/\text{d.o.f.}$  of all fits were between 0.8 ( $\langle M_H^2/s \rangle$ ) and 4.4 ( $\langle B_T \rangle$ ). We estimated the systematic uncertainties by varying  $x_\mu$  from 0.5 to 2 and  $\mu_I$  from 1 to 3 GeV.

The results of the fits are shown in Figure 3 and the numeric values are tabulated in Table 6. It presents the values for  $\alpha_s$  and for  $\bar{\alpha}_0$ , the experimental errors and systematic uncertainties of the fit results. We consider these results based on power corrections as a test of the new theoretical prediction [6]. It should be noted that the theoretically expected universality of  $\bar{\alpha}_0$  is observed only at the level of 30%.

Employing the procedure used in Section 4 to combine the individual  $\alpha_s$  values, we obtained

$$\alpha_s(M_{Z^0}) = 0.1188^{+0.0044}_{-0.0034}$$

where the error is the experimental uncertainty ( $\pm 0.0016$ ), the renormalisation scale uncertainty ( $^{+0.0033}_{-0.0023}$ ) and the uncertainty due to the choice of the infrared scale ( $^{+0.0024}_{-0.0019}$ ), all combined in quadrature. This result is in good agreement with the world average value [27] of  $\alpha_s^{\text{w.a.}}(M_{Z^0}) = 0.119 \pm 0.006$ .

## 6 Summary and Conclusions

Data recorded by the JADE experiment at centre-of-mass energies around 35 and 44 GeV were analysed in terms of event shape distributions.

The measured distributions were corrected for detector and initial state photon radiation effects using original Monte Carlo simulation data for 35 and 44 GeV. The simulated data are based on the JETSET parton shower generator version 6.3. The same event generator was also employed to correct the data for hadronisation effects in order to determine the strong coupling constant  $\alpha_s$ .

Our measurements of  $\alpha_s$  are based on the most complete theoretical calculations available to date. For all observables theoretical calculations exist in  $\mathcal{O}(\alpha_s^2)$  and in the next-to-leading log approximation. These two calculations were combined using the  $\ln(R)$ -matching scheme. We found the improved perturbative calculation of the jet broadening

to describe the data slightly better. With these calculations values of  $\alpha_s$  are obtained which are about 3% higher than previously. The  $\alpha_s$  values were also more consistent with those from other event shape observables.

Combining the values of  $\alpha_s$  obtained in this analysis with those from our previous publication and using the new values obtained from jet broadening, the final values at the two centre-of-mass energies are

$$\begin{aligned}\alpha_s(44 \text{ GeV}) &= 0.139 {}^{+0.011}_{-0.007} \\ \alpha_s(35 \text{ GeV}) &= 0.145 {}^{+0.012}_{-0.007},\end{aligned}$$

where the errors are formed by adding in quadrature the statistical, experimental systematics, Monte Carlo modelling and higher order QCD uncertainties. The dominant contributions to the total error came from the choice of the renormalisation scale and from uncertainties due to quark mass effects.

Evolving our  $\alpha_s$  measurements to  $\sqrt{s} = M_{Z^0}$  the results obtained at 35 and 44 GeV transform to  $0.123 {}^{+0.008}_{-0.005}$  and  $0.123 {}^{+0.008}_{-0.006}$ , respectively. The combination of these values gives  $\alpha_s(M_{Z^0}) = 0.123 {}^{+0.008}_{-0.005}$ .

The energy dependence of the mean values of the distributions can be directly compared with analytic QCD predictions plus power corrections for hadronisation effects involving an universal non-perturbative parameter  $\bar{\alpha}_0$  [6, 21]. Our studies resulted in

$$\alpha_s(M_{Z^0}) = 0.119 {}^{+0.004}_{-0.003}$$

which is in good agreement with our results from the  $\mathcal{O}(\alpha_s^2)$ +NLLA fits and also with the world average value. The universality of the non-perturbative parameter  $\bar{\alpha}_0$  is found only at a level of 30%.

## References

- [1] B. Naroska:  *$e^+e^-$  Physics with the JADE Detector at PETRA*, Phys. Rep. **148** (1987) 67.
- [2] P. Movilla Fernández, O. Biebel, S. Bethke, S. Kluth, P. Pfeifenschneider and the JADE collaboration: Eur. Phys. J. **C1** (1998) 461.
- [3] JADE Coll., W. Bartel et al.: Phys. Lett. **88B** (1979) 171.
- [4] Yu.L. Dokshitzer, A. Lucenti, G. Marchesini, G.P. Salam: *On the QCD analysis of Jet Broadening*, J. High Energy Phys. JHEP **01** (1998) 011, IFUM-602-FT, hep-ph/9801324.
- [5] S. Catani, B.R. Webber: *Resummed C-Parameter Distribution in  $e^+e^-$ -Annihilation*, CERN-TH/98-14, Cavendish-HEP-97/16, hep-ph/9801350.
- [6] Yu.L. Dokshitzer, A. Lucenti, G. Marchesini, G.P. Salam, Nucl. Phys. **B511** (1998) 396;  
Yu.L. Dokshitzer, A. Lucenti, G. Marchesini, G.P. Salam: *On the universality of the Milan factor for  $1/Q$  power corrections to jet shapes*, J. High Energy Phys. JHEP **05** (1998) 003, IFUM-601-FT, hep-ph/9802381;  
G.P. Salam: *The Milan factor for jet-shape observables*, IFUM-623-FT, hep-ph/9805323.
- [7] JADE Coll., W. Bartel et al.: Phys. Lett. **129B** (1983) 145.
- [8] JADE Coll., S. Bethke et al.: Phys. Lett. **B213** (1988) 235.
- [9] OPAL Coll., P.D. Acton et al.: Z. Phys. **C59** (1993) 1.
- [10] T. Sjöstrand: Comput. Phys. Commun. **39** (1986) 347;  
T. Sjöstrand, M. Bengtsson: Comput. Phys. Commun. **43** (1987) 367.
- [11] G. Parisi, Phys. Lett. **74B** (1978) 65;  
J.F. Donoghue, F.E. Low, S.Y. Pi, Phys. Rev. **D20** (1979) 2759.
- [12] JADE Coll., E. Elsen et al.: Z. Phys. **C46** (1990) 349.
- [13] OPAL Coll., G. Alexander et al.: Z. Phys. **C69** (1995) 543.
- [14] C. Peterson, D. Schlatter, I. Schmitt, P.M. Zerwas: Phys. Rev. D27 (1983) 105.
- [15] OPAL Coll., G. Alexander et al.: Z. Phys. **C72** (1996) 191.
- [16] OPAL Coll., P.D. Acton et al.: Z. Phys. **C55** (1992) 1.
- [17] R.K. Ellis, D.A. Ross, A.E. Terrano: Nucl. Phys. **B178** (1981) 421.
- [18] S. Catani, G. Turnock, B.R. Webber: Phys. Lett. **B295** (1992) 269.

- [19] Z. Kunszt, P. Nason, G. Marchesini, B.R. Webber: in *Z Physics at LEP 1*, vol. 1, ed. G. Altarelli, R. Kleiss and C. Verzegnassi, CERN Yellow Book 89-08.
- [20] We used the program EVENT2 of S. Catani and M.H. Seymour to determine the perturbative coefficients by integrating the ERT  $\mathcal{O}(\alpha_s^2)$  matrix elements [17]:  
S. Catani, M.H. Seymour: Phys. Lett. **B378** (1996) 287.
- [21] Yu.L. Dokshitzer, B.R. Webber: Phys. Lett. **B352** (1995) 451;  
B.R. Webber: proceedings of the *Workshop on Deep Inelastic Scattering and QCD (DIS 95)*, Paris, France, 24-28 Apr, 1995, ed. J.F. Laporte and Y. Sirois; Cavendish-HEP-95/11; hep-ph/9510283.
- [22] Yu.L. Dokshitzer, G. Marchesini, B.R. Webber: Nucl. Phys. **B469** (1996) 93.
- [23] L3 Coll., M. Acciarri et al.: Phys. Lett. **B404** (1997) 390.
- [24] OPAL Coll., K. Ackerstaff et al.: Z. Phys. **C75** (1997) 193.
- [25] ALEPH Coll., D. Buskulic et al.: Z. Phys. **C55** (1992) 209;  
ALEPH Coll., D. Buskulic et al.: Z. Phys. **C73** (1997) 409;  
AMY Coll., Y.K. Li et al.: Phys. Rev. **D41** (1990) 2675;  
DELCO Coll., M. Sakuda et al.: Phys. Rev. **152B** (1985) 399;  
DELPHI Coll., P. Abreu et al.: Z. Phys. **C73** (1996) 11;  
L3 Coll., B. Adeva et al.: Z. Phys. **C55** (1992) 39;  
L3 Coll., M. Acciarri et al.: Phys. Lett. **B371** (1996) 137;  
MarkII Coll., A. Peterson et al.: Phys. Rev. **D37** (1988) 1;  
MarkJ Coll., D.P. Barber et al.: Phys. Rev. Lett. **43** (1979) 901;  
MarkJ Coll., D.P. Barber et al.: Phys. Lett. **85B** (1979) 463;  
OPAL Coll., P.D. Acton et al.: Z. Phys. **C55** (1992) 1;  
OPAL Coll., G. Alexander et al.: Z. Phys. **C72** (1996) 191;  
SLD Coll., K. Abe et al.: Phys. Rev. **D51** (1995) 962;  
TASSO Coll., W. Braunschweig et al.: Z. Phys. **C41** (1988) 359;  
TASSO Coll., W. Braunschweig et al.: Z. Phys. **C47** (1990) 187.
- [26] DELPHI Coll., P. Abreu et al.: Z. Phys. **C73** (1997) 229.
- [27] S. Bethke: proceedings of the *QCD Euroconference 97*, Montpellier, France, July 3-9 (1997), Nucl. Phys. B (Proc. Suppl.) 64 (1998) 54-62; hep-ex/9710030.

## Tables

35 GeV	$1/\sigma \cdot d\sigma/dC$	44 GeV	$1/\sigma \cdot d\sigma/dC$
0.00-0.08	$0.064 \pm 0.004 \pm 0.034$	0.00-0.08	$0.093 \pm 0.008 \pm 0.031$
0.08-0.12	$0.434 \pm 0.019 \pm 0.079$	0.08-0.12	$0.801 \pm 0.047 \pm 0.131$
0.12-0.16	$1.383 \pm 0.039 \pm 0.068$	0.12-0.16	$1.953 \pm 0.086 \pm 0.250$
0.16-0.20	$2.436 \pm 0.056 \pm 0.068$	0.16-0.20	$3.016 \pm 0.116 \pm 0.189$
0.20-0.24	$2.678 \pm 0.060 \pm 0.229$	0.20-0.24	$3.172 \pm 0.123 \pm 0.288$
0.24-0.28	$2.845 \pm 0.062 \pm 0.260$	0.24-0.28	$2.759 \pm 0.116 \pm 0.141$
0.28-0.32	$2.289 \pm 0.054 \pm 0.208$	0.28-0.32	$2.457 \pm 0.108 \pm 0.286$
0.32-0.36	$2.327 \pm 0.056 \pm 0.269$	0.32-0.36	$1.748 \pm 0.086 \pm 0.098$
0.36-0.40	$1.837 \pm 0.047 \pm 0.109$	0.36-0.40	$1.623 \pm 0.082 \pm 0.230$
0.40-0.44	$1.441 \pm 0.041 \pm 0.131$	0.40-0.44	$1.163 \pm 0.068 \pm 0.150$
0.44-0.48	$1.254 \pm 0.038 \pm 0.066$	0.44-0.48	$1.159 \pm 0.070 \pm 0.210$
0.48-0.52	$1.024 \pm 0.034 \pm 0.071$	0.48-0.52	$0.847 \pm 0.056 \pm 0.071$
0.52-0.58	$0.839 \pm 0.025 \pm 0.034$	0.52-0.58	$0.720 \pm 0.041 \pm 0.070$
0.58-0.64	$0.702 \pm 0.022 \pm 0.095$	0.58-0.64	$0.626 \pm 0.038 \pm 0.046$
0.64-0.72	$0.532 \pm 0.017 \pm 0.030$	0.64-0.72	$0.503 \pm 0.030 \pm 0.050$
0.72-0.82	$0.453 \pm 0.014 \pm 0.051$	0.72-0.82	$0.348 \pm 0.022 \pm 0.034$
0.82-1.00	$0.090 \pm 0.004 \pm 0.010$	0.82-1.00	$0.079 \pm 0.008 \pm 0.015$
mean value	$0.3673 \pm 0.0013 \pm 0.0040$	mean value	$0.3404 \pm 0.0023 \pm 0.0037$

Table 3: Event shape data at  $\sqrt{s} = 35$  (left) and 44 GeV (right) for the  $C$ -parameter observable. The values were corrected for detector and for initial state radiation effects. The first error denotes the statistical and the second the experimental systematic uncertainty.

	$B_T$	$B_W$	$C$
$\alpha_s(44 \text{ GeV})$	<b>0.1458</b>	<b>0.1318</b>	<b>0.1470</b>
fit range	0.08-0.27	0.06-0.16	0.16-0.64
$\chi^2/\text{d.o.f.}$	3.1	11.5	1.8
Statistical error	$\pm 0.0014$	$\pm 0.0016$	$\pm 0.0017$
tracks only	-0.0027	-0.0004	-0.0018
clusters only	+0.0009	+0.0015	+0.0015
$\cos \theta_t$	$\pm 0.0005$	$\pm 0.0008$	$\pm 0.0004$
$p_{\text{miss}}$	$\pm 0.0001$	$\pm 0.0002$	$\pm 0.0003$
$p_{\text{bal}}$	$\pm 0.0002$	$\pm 0.0004$	$\pm 0.0003$
$N_{\text{ch}}$	+0.0003	+0.0003	+0.0003
$E_{\text{vis}}$	$\pm 0.0003$	$\pm 0.0002$	$\pm 0.0005$
fit range	$\pm 0.0023$	$\pm 0.0047$	$\pm 0.0019$
Experimental syst.	$\pm 0.0037$	$\pm 0.0051$	$\pm 0.0027$
$a - 0.225$	+0.0017	+0.0010	+0.0026
$a + 0.225$	-0.0017	-0.0009	-0.0027
$\sigma_q - 30 \text{ MeV}$	+0.0009	+0.0007	+0.0014
$\sigma_q + 30 \text{ MeV}$	-0.0010	-0.0006	-0.0014
LUND symmetric	+0.0017	+0.0015	+0.0025
$Q_0 + 500 \text{ MeV}$	-0.0007	+0.0012	-0.0007
$Q_0 - 500 \text{ MeV}$	+0.0002	-0.0002	+0.0002
$\Lambda - 50 \text{ MeV}$	-0.0013	+0.0001	-0.0015
$\Lambda + 50 \text{ MeV}$	+0.0008	< 0.0001	+0.0010
udsc only	+0.0064	+0.0047	+0.0058
MC statistics	$\pm 0.0008$	$\pm 0.0009$	$\pm 0.0011$
MC modelling	+0.0072 -0.0032	+0.0054 -0.0026	+0.0073 -0.0044
$x_\mu = 0.5$	-0.0100	-0.0061	-0.0107
$x_\mu = 2.0$	+0.0127	+0.0081	+0.0133
Total error	+0.0151 -0.0112	+0.0111 -0.0085	+0.0155 -0.0120

Table 4: Values of  $\alpha_s(44 \text{ GeV})$  derived using the  $\mathcal{O}(\alpha_s^2)$ +NLLA QCD calculations with  $x_\mu = 1$  and the  $\ln(R)$ -matching scheme, fit ranges and  $\chi^2/\text{d.o.f.}$  values for each of the three event shape observables. In addition, the statistical and systematic uncertainties are given. Where a signed value is quoted, this indicates the direction in which  $\alpha_s(44 \text{ GeV})$  changed with respect to the standard analysis. The scale uncertainty and quark mass effects are treated as asymmetric uncertainties of  $\alpha_s$ .

	$B_T$	$B_W$	$C$
$\alpha_s(35 \text{ GeV})$	<b>0.1489</b>	<b>0.1367</b>	<b>0.1480</b>
fit range	0.08-0.27	0.06-0.16	0.16-0.64
$\chi^2/\text{d.o.f.}$	3.1	4.1	2.7
Statistical error	$\pm 0.0008$	$\pm 0.0009$	$\pm 0.0009$
tracks only	-0.0010	-0.0006	-0.0011
clusters only	-0.0009	-0.0018	-0.0007
$\cos \theta_T$	$\pm 0.0001$	$\pm 0.0002$	$\pm 0.0002$
$p_{\text{miss}}$	$\pm 0.0001$	$\pm 0.0003$	$\pm 0.0002$
$p_{\text{bal}}$	$\pm 0.0002$	$\pm 0.0006$	$\pm 0.0002$
$N_{\text{ch}}$	$+0.0005$	$+0.0006$	$+0.0007$
$E_{\text{vis}}$	$\pm 0.0001$	$\pm 0.0001$	$\pm 0.0001$
fit range	$\pm 0.0008$	$\pm 0.0016$	$\pm 0.0004$
Experimental syst.	$\pm 0.0014$	$\pm 0.0026$	$\pm 0.0014$
$a - 0.225$	$+0.0023$	$+0.0018$	$+0.0037$
$a + 0.225$	-0.0021	-0.0020	-0.0030
$\sigma_q - 30 \text{ MeV}$	$+0.0013$	$+0.0015$	$+0.0017$
$\sigma_q + 30 \text{ MeV}$	-0.0012	-0.0013	-0.0015
LUND symmetric	$+0.0027$	$+0.0029$	$+0.0031$
$Q_0 + 500 \text{ MeV}$	-0.0014	$+0.0014$	-0.0004
$Q_0 - 500 \text{ MeV}$	$+0.0006$	-0.0008	$+0.0001$
$\Lambda - 50 \text{ MeV}$	-0.0021	-0.0003	-0.0024
$\Lambda + 50 \text{ MeV}$	$+0.0018$	$+0.0003$	$+0.0020$
udsc only	$+0.0086$	$+0.0077$	$+0.0078$
MC statistics	$\pm 0.0007$	$\pm 0.0008$	$\pm 0.0008$
MC modelling	$+0.0099$ $-0.0048$	$+0.0089$ $-0.0045$	$+0.0097$ $-0.0058$
$x_\mu = 0.5$	-0.0107	-0.0075	-0.0110
$x_\mu = 2.0$	$+0.0136$	$+0.0096$	$+0.0138$
Total error	$+0.0169$ $-0.0119$	$+0.0134$ $-0.0091$	$+0.0169$ $-0.0126$

Table 5: Values of  $\alpha_s(35 \text{ GeV})$  derived as in Table 4 but at 35 GeV.

(a)	$\langle 1 - T \rangle$	$\langle M_H^2/s \rangle$	$\langle B_T \rangle$	$\langle B_W \rangle$	$\langle C \rangle$	average
$\alpha_s(M_{Z^0})$	<b>0.1197</b>	<b>0.1140</b>	<b>0.1211</b>	<b>0.1217</b>	<b>0.1201</b>	<b>0.1188</b>
$Q$ range [GeV]	13-172	14-172	35-172	35-172	35-172	
$\chi^2/\text{d.o.f.}$	43.2/24	12.1/16	38.9/9	21.6/9	11.0/7	
experimental	$\pm 0.0013$	$\pm 0.0010$	$\pm 0.0020$	$\pm 0.0020$	$\pm 0.0016$	$\pm 0.0016$
$x_\mu = 0.5$	-0.0050	-0.0026	-0.0039	-0.0002	-0.0046	-0.0023
$x_\mu = 2.0$	+0.0061	+0.0037	+0.0049	+0.0011	+0.0057	+0.0033
$\mu_I = 1$ GeV	+0.0026	+0.0013	+0.0044	+0.0027	+0.0025	+0.0024
$\mu_I = 3$ GeV	-0.0020	-0.0011	-0.0036	-0.0021	-0.0020	-0.0019
Total error	+0.0068 -0.0055	+0.0040 -0.0030	+0.0069 -0.0057	+0.0035 -0.0029	+0.0064 -0.0053	+0.0044 -0.0034

(b)	$\langle 1 - T \rangle$	$\langle M_H^2/s \rangle$	$\langle B_T \rangle$	$\langle B_W \rangle$	$\langle C \rangle$
$\bar{\alpha}_0$	<b>0.510</b>	<b>0.616</b>	<b>0.396</b>	<b>0.325</b>	<b>0.443</b>
experimental	$\pm 0.012$	$\pm 0.018$	$\pm 0.019$	$\pm 0.020$	$\pm 0.011$
$x_\mu = 0.5$	+0.004	+0.012	+0.005	+0.082	+0.006
$x_\mu = 2.0$	-0.002	-0.005	-0.001	-0.036	-0.003
Total error	+0.013 -0.012	+0.022 -0.019	+0.020 -0.019	+0.084 -0.041	+0.013 -0.011

Table 6: Values of  $\alpha_s(M_{Z^0})$  (a) and  $\bar{\alpha}_0$  (b) derived using  $\mu_I = 2$  GeV and  $x_\mu = 1$  and the  $\mathcal{O}(\alpha_s^2)$  calculations and two-loop power corrections which include the Milan factor [6]. Fit ranges and  $\chi^2/\text{d.o.f.}$  values for each of the five event shape observables are specified. In addition, the statistical and systematic uncertainties are given. Where a signed value is quoted, this indicates the direction in which  $\alpha_s(M_{Z^0})$  and  $\bar{\alpha}_0$  changed with respect to the standard analysis. The renormalisation and infrared scale uncertainties are treated as an asymmetric uncertainty on  $\alpha_s(M_{Z^0})$ . These uncertainties are treated equally for  $\bar{\alpha}_0$  but exclude the infrared scale uncertainty.

## Figures

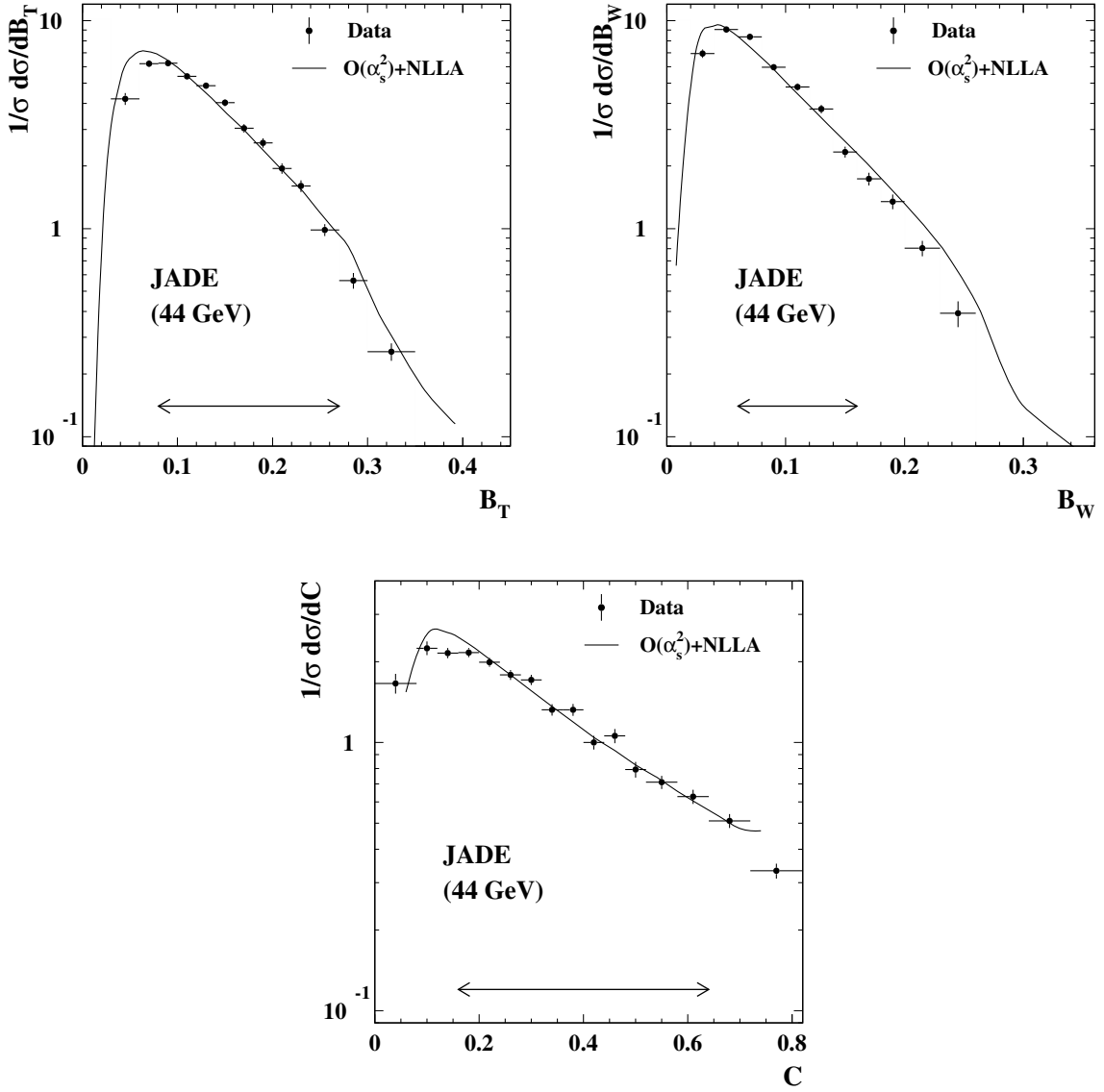


Figure 1: Distributions measured at  $\sqrt{s} = 44$  GeV and corrected to parton level are shown for the total and wide jet broadening  $B_T$  and  $B_W$  and for the  $C$ -parameter. The fits, using the improved  $\mathcal{O}(\alpha_s^2) + \text{NLLA}$  QCD prediction for the jet broadening are overlayed and the fit ranges are indicated by the arrows. The error bars represent statistical errors only.

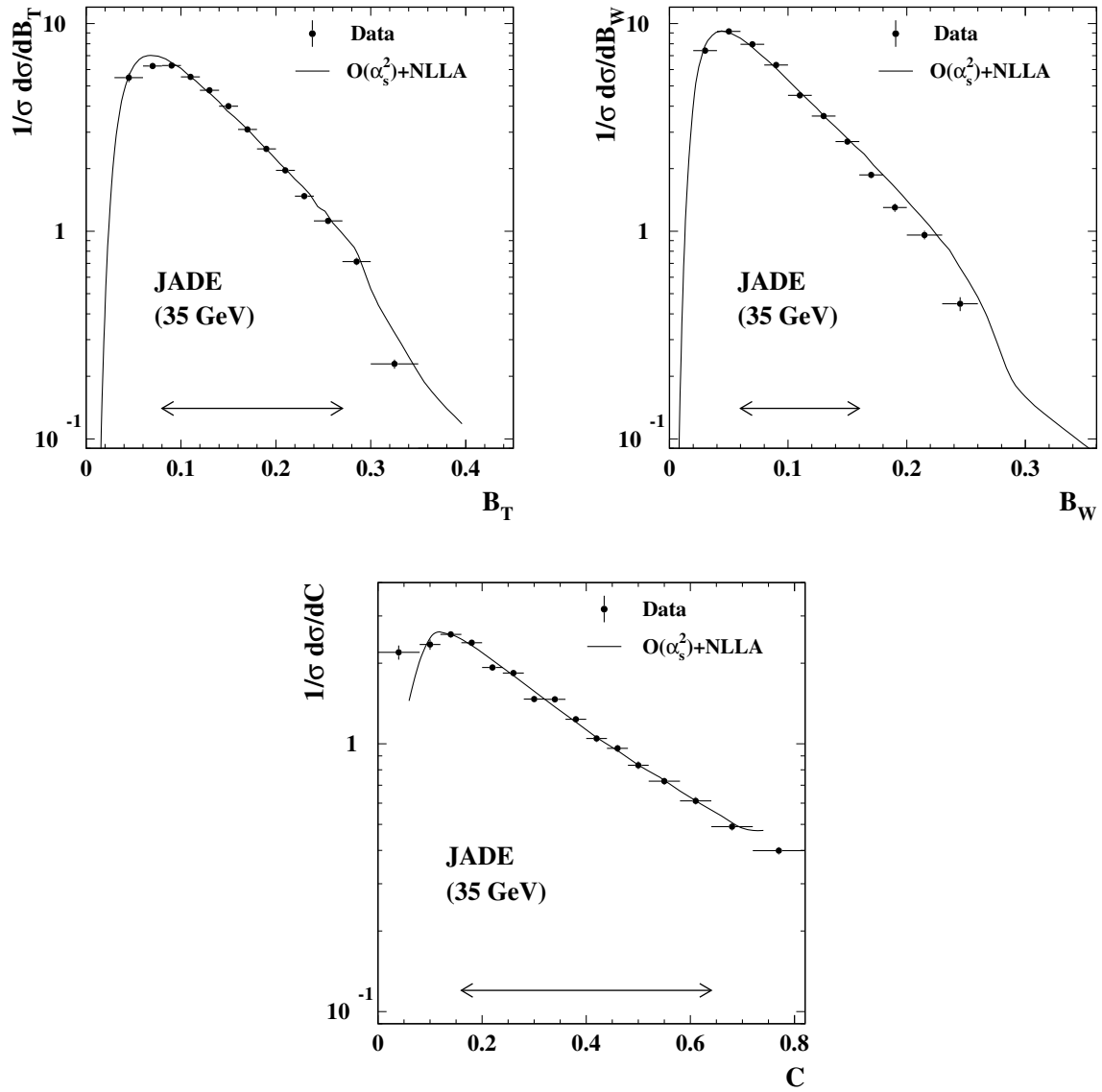


Figure 2: The same distributions as in Figure 1 but for  $\sqrt{s} = 35$  GeV.

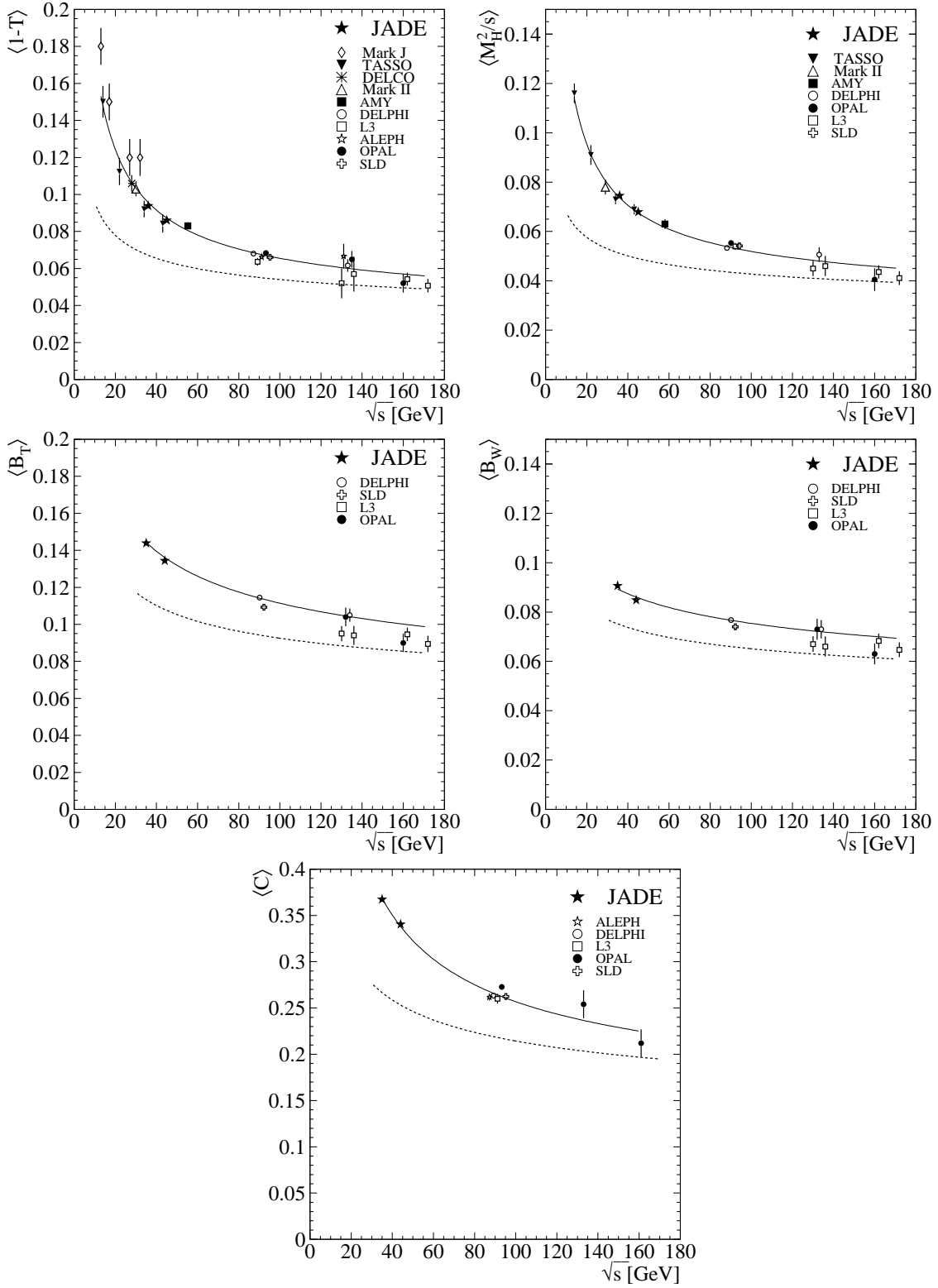


Figure 3: Energy dependence of the mean values of thrust  $\langle 1-T \rangle$ , heavy jet mass  $\langle M_H^2/s \rangle$ , total  $\langle B_T \rangle$  and wide jet broadening  $\langle B_W \rangle$ , and of the  $C$ -parameter  $\langle C \rangle$  are shown [23–26]. The solid curve is the result of the fit using perturbative calculations plus two-loop power corrections which include the Milan factor [6] while the dashed line is the perturbative prediction for the same value of  $\alpha_s(M_{Z^0})$ .